

Characteristics of AA6061/BN Composite Fabricated by Pressureless Infiltration Technique

KON BAE LEE, JAE PYOUNG AHN and HOON KWON

Spontaneous infiltration and strengthening behaviors were analyzed in terms of microstructures and tensile properties of AA6061/BN composite fabricated by pressureless infiltration technique in the presence of both Mg and nitrogen. The microstructure and properties were compared with control AA6061 without BN fabricated by the same method. The Mg_3N_2 formed by the reaction of Mg vapor and nitrogen gas, which coated the particles in the powder bed, is believed to induce spontaneous infiltration through greatly enhancing wetting by means of the reaction $Mg_3N_2 + 2Al \rightarrow 2AlN + 3Mg$. This was identified by the finding of AlN particle layers on the surfaces of prior Al particles in the powder bed, which made contact with the infiltrating melt. In addition, unreacted Mg_3N_2 was observed outside the composite, where the Al melt did not come into direct contact. Fine AlN particles formed *in situ* resulted in significant strengthening, even in the control alloy, with no addition of BN. In the composite reinforced with BN, additional AlN was formed by the interfacial reaction of the BN and Al melt as well as by the *in situ* reaction. Consequently, both the BN particles and the additional AlN particles formed by the interfacial reaction led to a further strengthening in the composite, as compared to the control alloy, which was strengthened only by the AlN particles formed *in situ*. In addition, the flake shape of BN may have lent considerable strength, due to the high aspect ratio it demonstrates, as compared with that of a spherically shaped particle.

I. INTRODUCTION

METAL matrix composites (MMCs) reinforced with ceramic phase have become of great interest because of the combined effects of metallic and ceramic materials relative to the corresponding monolithic alloys. Thus, various fabrication methods have been developed, such as powder metallurgy, stir casting, pressure infiltration method, *etc.* Furthermore, in recent years there has been a growing interest in the development of technologies for the *in situ* production of MMCs, such as Lanxide's PRIMEX* process, Martin

*PRIMEX is a trademark of Lanxide.

Marietta's XD** process, self-propagating high-temperature

**XD is a trademark of Martin Marietta.

synthesis (SHS) and reactive-gas injection.^[1-10]

Many kinds of ceramic phases have been added as a reinforcement in Al matrix composites: particles, whiskers and fibers of the oxides (Al_2O_3 , MgO, TiO_2 , *etc.*), carbides (SiC , TiC , B_4C , *etc.*), nitrides (AlN, BN, Si_3N_4 , *etc.*), and borides (TiB_2 , *etc.*). Boron nitride (BN) is an interesting material because of its unique combination of properties, such as its low density, high melting point, high thermal conductivity, and high electrical resistivity.^[11,12] There are many reports that the BN/Al system shows much better wettability than several other ceramic/metal systems.^[13-18]

KON BAE LEE, Professor, is with the School of Metallurgical and Materials Engineering, Kookmin University, Seoul 136-702, Korea. JAE PYOUNG AHN, Postdoctor, is with the Materials Science Division, Lawrence Berkeley Laboratory, Berkeley, CA 94720. HOON KWON, Professor, School of Metallurgical and Materials Engineering, Kookmin University, is jointly appointed at the Center for Advanced Aerospace Materials, POSTECH, Pohang 790-784, Korea.

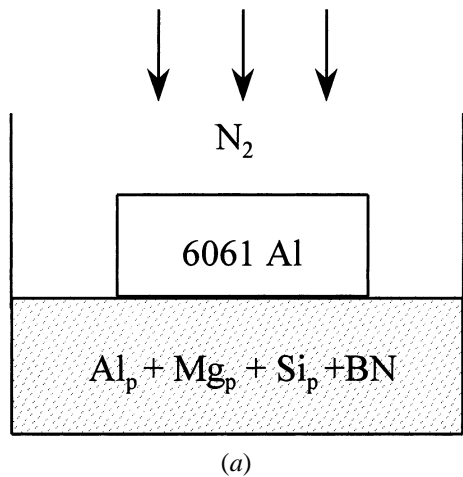
Manuscript submitted February 28, 2000.

Fujii *et al.*,^[13] in particular, reported that the equilibrium contact angle was 0 deg at 1000 °C. Thus, they suggested that BN might be an optimum material to be reinforced into an Al matrix, from the standpoint of wetting. However, since most of the work on the BN/Al system has been focused on wettability and on the an interfacial reaction between BN and Al, and not on its real bulk composites, its mechanical properties are rarely, if ever, known. Therefore, an Al composite reinforced with BN was fabricated by the pressureless infiltration method in this study in order to investigate its characteristics.

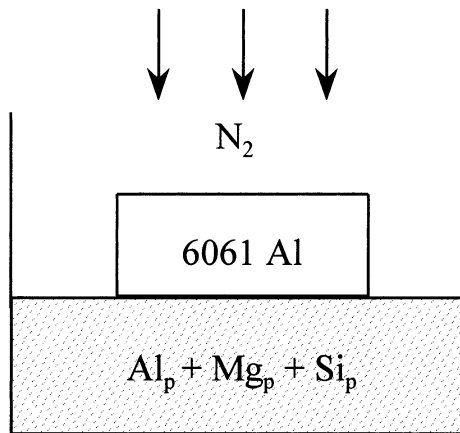
The PRIMEX process is an innovative technique for fabricating MMCs by the spontaneous infiltration of molten Al alloy containing Mg into a ceramic filler or preform under a nitrogen atmosphere, without the aid of vacuum or externally applied pressure.^[5-10]

For the pressureless infiltration in this process, both nitrogen and Mg are needed. Previous studies have investigated that the spontaneous infiltration of molten Al alloy, in providing the matrix of Al composites in this process, is influenced by Mg content, additional alloying elements, nitrogen concentration in the gas atmosphere, infiltration temperature and time, *etc.*^[5-10] Specifically, at least 1 wt pct, and preferably 3 wt pct, Mg is required.

Recently, Lee and co-workers^[19,20] have given attention to ceramic particle reinforced composites with lower Mg matrix content similar to 6061, fabricated by pressureless infiltration. In addition, their previous studies^[21] showed that control alloys, such as AA5052, 5083, 6061, and 7075, without artificial reinforcement and fabricated by the same process, basically differed from corresponding commercial Al alloys, and were really composites reinforced with self-made AlN particles, *i.e.*, a kind of *in-situ* composite. Thus, these control alloys exhibited considerable strengthening, as compared to the monolithic commercial Al alloys produced by conventional methods.



(a)



(b)

Fig. 1—Schematic of the infiltration experiment: (a) composite and (b) control alloy.

This study describes the characteristics of AA6061/BN composite fabricated by the pressureless infiltration method, comparing the control AA6061 fabricated by the same method in order to understand the basic spontaneous infiltration and strengthening mechanisms.

II. EXPERIMENTAL PROCEDURE

Figure 1 shows the schematic arrangement employed for composite and control alloy fabrication in this study. For composite fabrication, the bottom part of the assembly was filled with (Al_p -1.2 wt pct Mg_p -0.8 wt pct Si_p)/ BN_p loose powder mixture, which was prepared by roll mixing in an alumina jar for 10 hours. A 6061 Al ingot was then placed on this powder bed. The average sizes of the Al, Mg, and Si particles were about 50, 13, and 20 μm , respectively. The BN particles supplied by Cerac Inc. (Milwaukee, WI) were hcp-BN of flake type, average thickness, and 0.8 μm (Figure 2) their volume fraction in the powder mixture bed for the composite fabrication was 5 pct. The assembly was heated up to 800 °C and held for 1 hour under flowing nitrogen atmosphere in the retort furnace. For comparison, the control AA6061 was made through the same route, using a powder bed without the BN. Both of these ingots were extruded at 450 °C into a bar 16 mm in diameter (extrusion ratio 22:1).

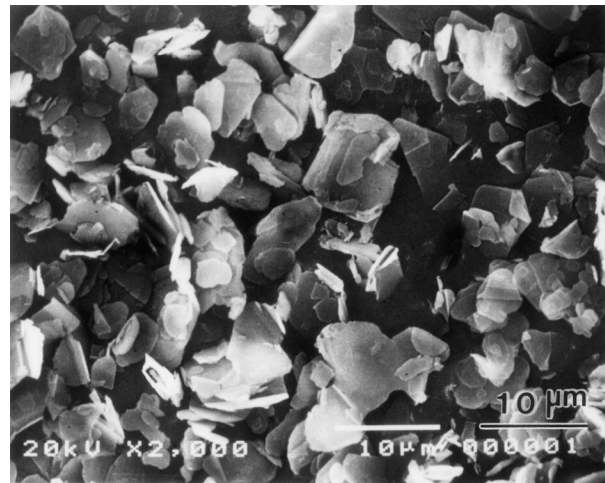


Fig. 2—SEM micrograph of BN flakes.

Tensile specimens having a gage length of 25 and 2 mm thickness were machined from the extruded bars, parallel to the extrusion direction. Those specimens were heat treated to the T6 condition (529 °C, 2-hour solution treatment, water quenching, and 177 °C, aging for 6 to 8 hours). Tensile testing was performed at room temperature, using a crosshead speed of 1 mm/min. Average tensile data were obtained from at least five tests for each condition.

The resulting microstructures and reaction products were investigated using X-ray diffraction (XRD), scanning electron microscopy (SEM), transmission electron microscopy (TEM), and Auger electron spectroscopy (AES). For the SEM analysis of the reaction products, specimens were prepared by dissolving away the metal matrix in a solution of methanol bromine and examined using a JEOL* 1210LV

*JEOL is a trademark of Japan Electron Optics Ltd., Tokyo.

SEM equipped with an energy dispersive X-ray spectrometer (EDS) operated at 20 kV. Thin foils for TEM analysis were ground mechanically to a thickness of about 60 μm and then punched into discs 3 mm in diameter. Finally, the discs were thinned using dimpling and ion milling (5 kV, at a tilt angle of 5 to 12 deg). All samples were examined by JEOL 1210 and JEOL 2010 TEM coupled to an EDS system operated at 120 and 200 kV, respectively.

III. EXPERIMENTAL RESULTS

A. Microstructural Analysis

Figure 3 shows the XRD spectra of commercial AA6061, control AA6061, and composite reinforced with BN. As expected, the commercial alloy presented the peaks corresponding only to Al. In contrast, the control alloy exhibited the additional small peaks of AlN. This means that the AlN was formed *via* the *in situ* reaction within the system during the fabrication of control AA6061. The composite reinforced with BN showed the higher peaks of AlN as well as the peaks of BN.

Figure 4 shows secondary electron images and elemental dot-mapping images of control alloy and composite in the as-fabricated condition prior to extrusion. It can be seen that

N is enriched, but Al is deficient on the surface of the old Al particles that had comprised the powder bed prior to infiltration, as compared to their interior. Of course, B and N were detected from the BN reinforcement in the composite. When compared with the XRD results, a main reaction product is identified as AlN in both control alloy and composite. The most important concern is where the AlN is formed, that is, mostly on the Al particle surface, where the infiltrating melt directly comes into contact. This will be discussed later.

Figure 5 shows secondary electron images and EDS and AES spectra of the reaction product obtained in the control alloy after dissolving away the Al alloy matrix with a solution of methanol bromine. A great amount of reaction product (the size of which about 1.0 μm) was clearly observed

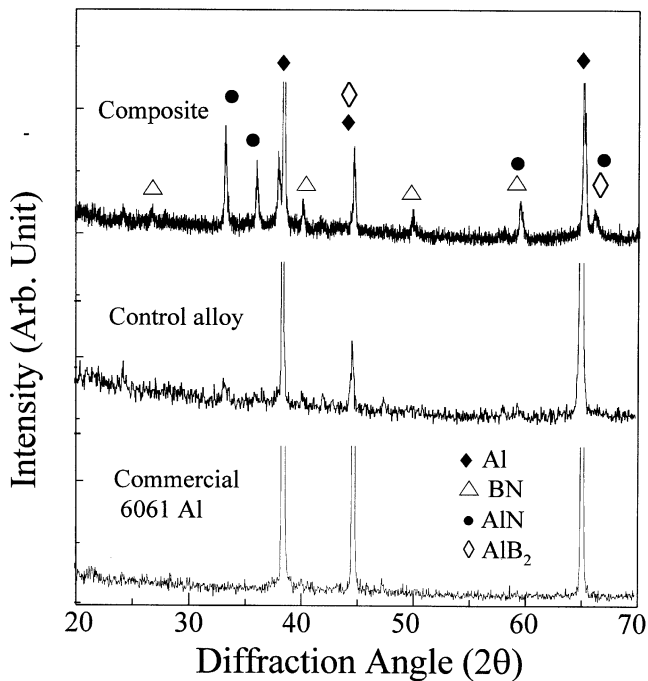


Fig. 3—XRD profile of the commercial AA6061, control alloy, and composite.

on the surface of the old Al particles that had comprised the powder bed prior to infiltration. After extrusion, this was, of course, aligned along the extrusion direction, as shown in Figure 5(b). Analyses by AES and EDS revealed only Al and N; the atomic ratio of Al to N was around 1, coincident with the stoichiometry of AlN. Figure 6 shows bright-field (BF) and dark-field (DF) images, and selected area diffraction patterns (SADPs) of the reaction product observed by TEM in both control alloy and composite. This reaction product was identified as AlN with a hexagonal structure and lattice parameters, $a = 3.093 \text{ nm}$ and $c = 5.046 \text{ nm}$ in the control alloy, and $a = 3.077 \text{ nm}$ and $c = 4.882 \text{ nm}$ in the composite (theoretical value $a = 3.1114 \text{ nm}$ and $c = 4.9792 \text{ nm}$, space group: $P6_3mc$).^[22] Phases identified from SADP were also confirmed using convergent beam electron diffraction (CBED) patterns (Figure 7). These analytical results obtained from CBED patterns are summarized in Table I.

Figure 8 shows SEM micrographs and AES and EDS spectra of another reaction product observed in both the control alloy and composite. According to the analytical results obtained from both EDS and AES analyses (Figures 8(c) and (d)), the particle of polyhedron morphology was identified as MgAl_2O_4 . Oxide films on Al and BN particles in the powder mixture can provide a source of oxygen for formation of MgAl_2O_4 . Phases identified from both EDS and AES analyses were also confirmed using TEM. Figure 9 shows the BF and DF images, and SADPs of the reaction product observed in the control alloy and composite, respectively. The reaction product was identified as the MgAl_2O_4 of cubic structure with the measured lattice parameter, $a = 8.100$ and 7.977 nm (theoretical value: 8.0831 nm , space group: $Fd3m$).^[22] Phases identified from SADPs were also confirmed using CBED patterns (Figure 7). Analytical results obtained from CBED patterns are summarized in Table I.

Figure 10 shows the reaction product and its EDS and AES spectra observed only in the composite reinforced with BN (after dissolving the Al matrix with a solution of methanol bromine). It was seen that the reaction product was AlB_2 which coarsely grew into a rectangular morphology. While

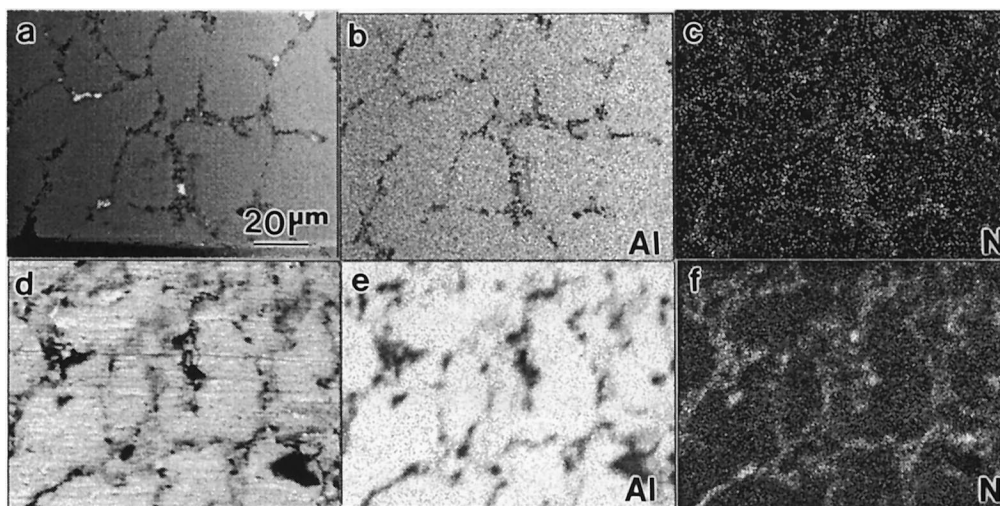


Fig. 4—Secondary electron images and elemental dot-mapping images observed by EDS at the polished surface in the as-fabricated condition: (a) through (c) in the control alloy and (d) through (f) in the composite, respectively.

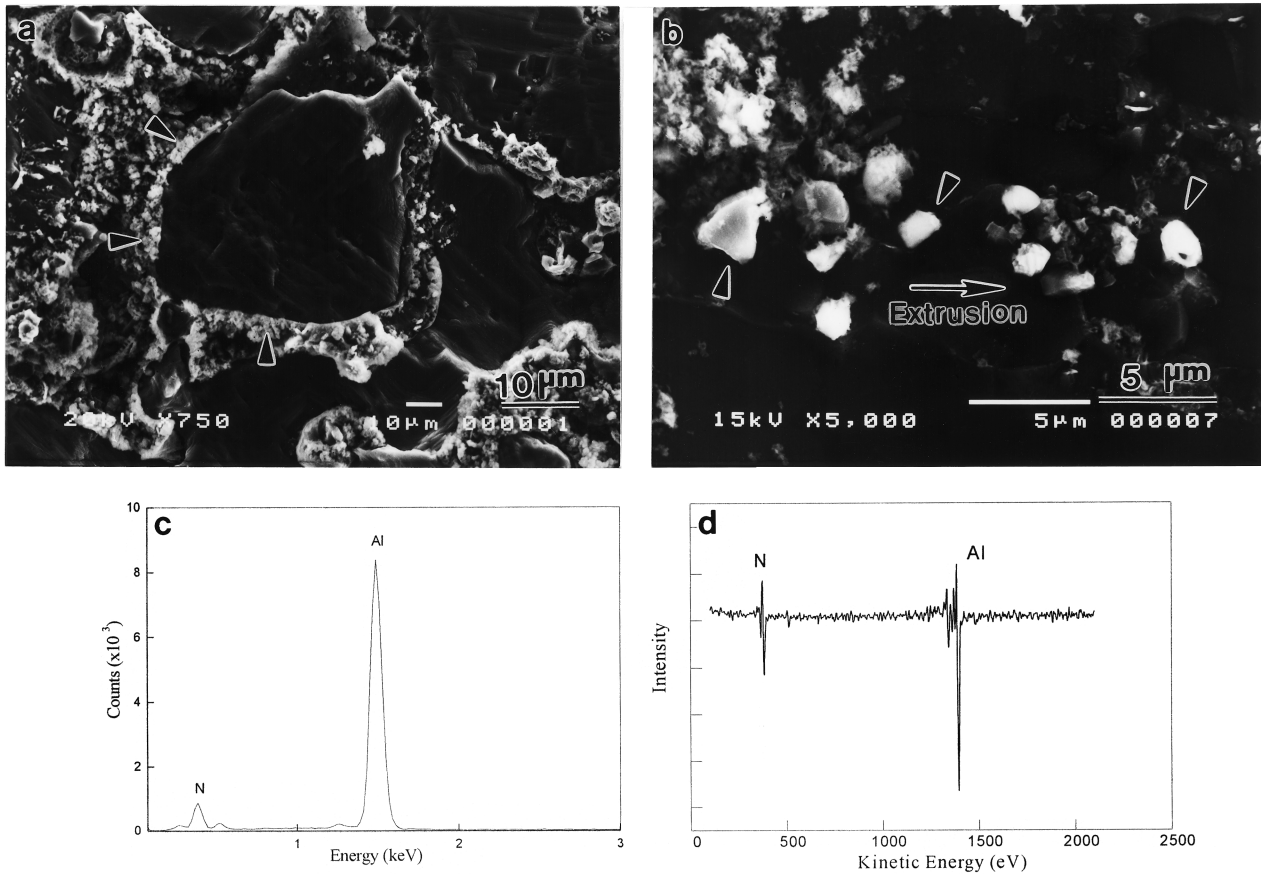


Fig. 5—SEM micrographs, EDS, and AES spectra showing the AlN reaction products, after dissolving away the Al alloy matrix in the control alloy: (a) as-fabricated and (b) extruded condition.

the EDS used in this study is capable of detecting elemental boron (B), this was not detected from the reaction product, as shown in Figure 10. It was not possible to detect simultaneously the Al, Mg, and B, due to excessive correction factors for atomic number and absorption.^[23] Using AES analysis, however, elemental boron was detected from the same reaction products. The specific reaction products containing aluminum, magnesium, and boron, were Al(Mg)-boride. Figure 11 shows the BF and DF images and SADPs of the reaction product observed in the composite. The reaction product AlB_2 was identified as having a hexagonal structure with measured lattice parameters of $a = 3.02$ nm, $c = 3.289$ nm (theoretical value; $a = 3.0054$ nm, $c = 3.25276$ nm, space group: $P6/mmm$).^[22] To confirm the result obtained from SADP analysis, we measured the primitive cell volume and the height of the reciprocal lattice from the CBED pattern (Figure 7 and Table I). That reaction product was identified as Al boride containing Mg with AlB_2 structure. Figure 12 shows the BF image and lattice image of the reaction product (AlB_2) observed by high-resolution TEM.

Figure 13 shows the BF and DF images and SADPs of BN with a hexagonal structure with measured lattice parameters of $a = 2.50441$ nm, $c = 6.6562$ nm (theoretical value, $a = 2.553$ nm, $c = 2.50441$ nm, space group: $P6_3/mmc$).^[22]

B. Tensile Properties

Figure 14 and Table II show the variation of tensile strength with aging time at 177 °C in commercial AA6061,

control AA6061, and composites that were solution treated for 2 hours at 529 °C. The tensile strength in the control AA6061 was 55 to 70 MPa greater than the commercial AA6061. These values were an additional 50 to 90 MPa higher in the composite reinforced with BN, compared to the control alloy. A large increase in strength in the case of the control AA6061 is related to the *in-situ* formation of AlN particles. In the composite reinforced with BN, AlN was formed by the direct reaction at the interface of BN and Al melt as well as by the *in-situ* reaction. Hence, a further increase in the strength of the composite, as compared to the control AA6061, is very likely attributable to both the fine reinforcing BN particles and the fine additional AlN particles formed by the interfacial reaction between BN and Al melt. In addition, since aging kinetics were accelerated by the formation of AlN as well as by the addition of BN, the time to peak strength decreased in both control alloy and composite. The grain size was measured by the linear intercept method. Even though the grain size is not uniform, the grain sizes of commercial, control, and composite are about 50, 20, and 3 μm, respectively.

IV. DISCUSSION

A. Infiltration Behavior

The spontaneous infiltration of molten metal at 800 °C for 1 hour under a nitrogen atmosphere made it possible to

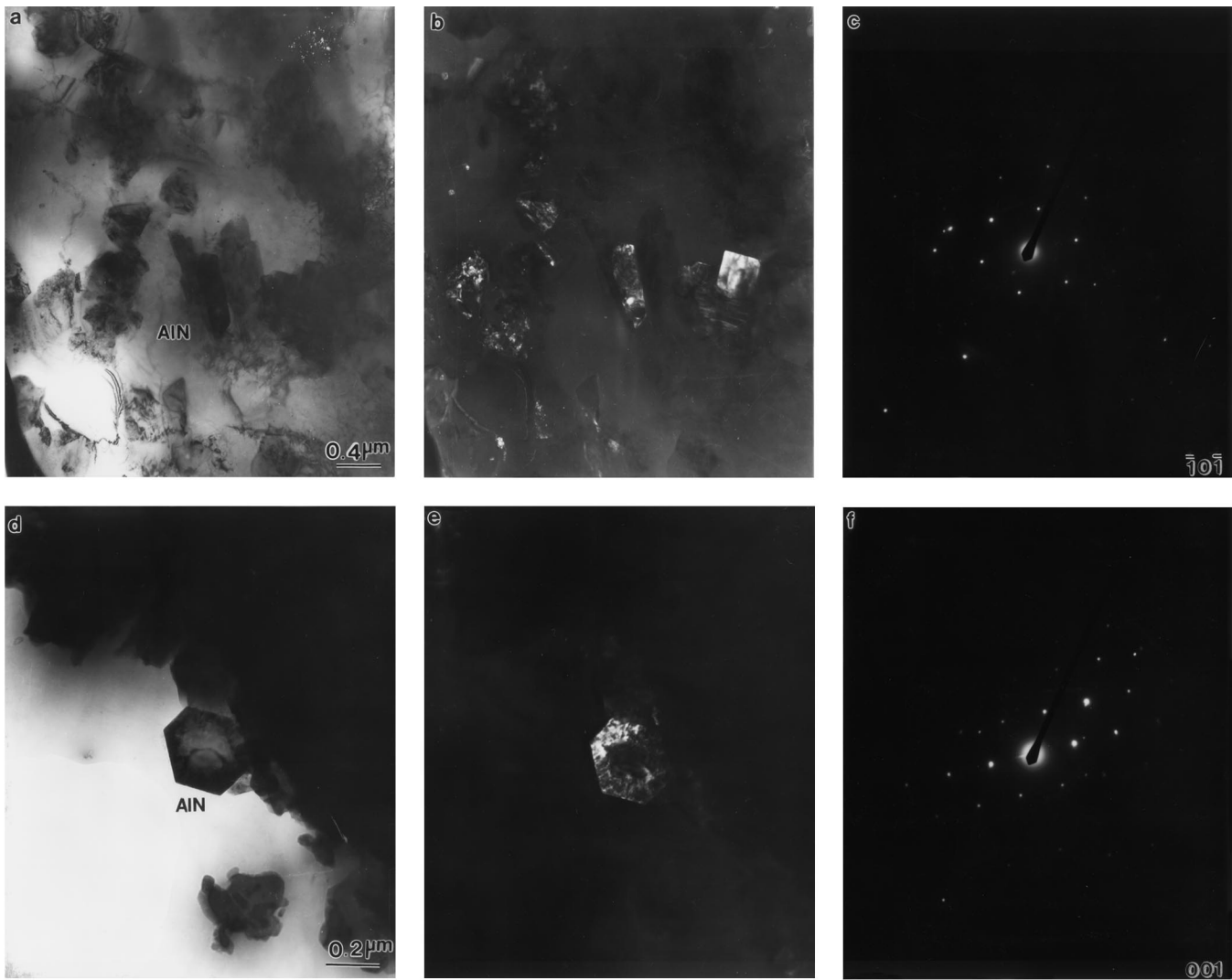


Fig. 6—TEM micrographs showing reaction products, AlN: (a) BF, (b) DF, and (c) SADP in control alloy and (d) BF, (e) DF, and (f) in the composite, respectively.

fabricate 6061 Al matrix composite reinforced with BN, as well as control 6061 Al without BN. When considering the melting point of Al, 667 °C, which is much lower than 800 °C, it seems surprising that the powder bed, consisting of almost all Al particles, sustains its shape and does not melt down, even at 800 °C. Al particles are not broken down, even at 800 °C, because the very thin oxide film on their surface may play a role as a barrier, keeping the molten Al in the particle from flowing out. Then the melt of alloy on the powder bed can infiltrate into interstices, in contact with the particle surface of the powder bed. Therefore, the as-fabricated microstructure may give a significant clue in elucidating the spontaneous infiltration mechanism in the presence of both Mg and nitrogen, since those contacting interfaces can be preserved only before extrusion. In particular, the analysis of the reaction products formed on the original Al particle surface has an important meaning. In other words, while any other excessive reaction on the ceramic particle surface requires the main reaction in order to induce the spontaneous infiltration vague, those reactions may not occur on the original Al particle surface.

Thus, the AlN appears to be a resultant reaction product that could be key to solving the spontaneous infiltration process in the presence of both Mg and N. In the control alloy, AlN was formed by the *in-situ* reaction mostly on the Al particle surface during the fabrication. On the other hand, an additional AlN was formed both by the interfacial reaction of the BN and Al melt, and *in situ*.

Table III shows the contact angles between BN and Al reported in literature. Even though BN and molten Al showed good wettability compared to other ceramic/Al systems, the wetting angles measured at 800 °C were in the range of 150 to 160 deg. This indicates that poor wetting may occur between the Al melt and the BN at 800 °C, as in the overall ceramic/Al systems. Hence, the fact that the spontaneous infiltration of molten metal can occur in the PRIMEX process is a very interesting and important phenomenon.

Aghajanian *et al.*^[10] suggested that Mg vapor (serving as an infiltration enhancer precursor) reacts with nitrogen to form Mg₃N₂ coatings (which serve as an infiltration enhancer) around the particles in the preform or filler. This Mg₃N₂ may lead to a spontaneous infiltration of molten Al

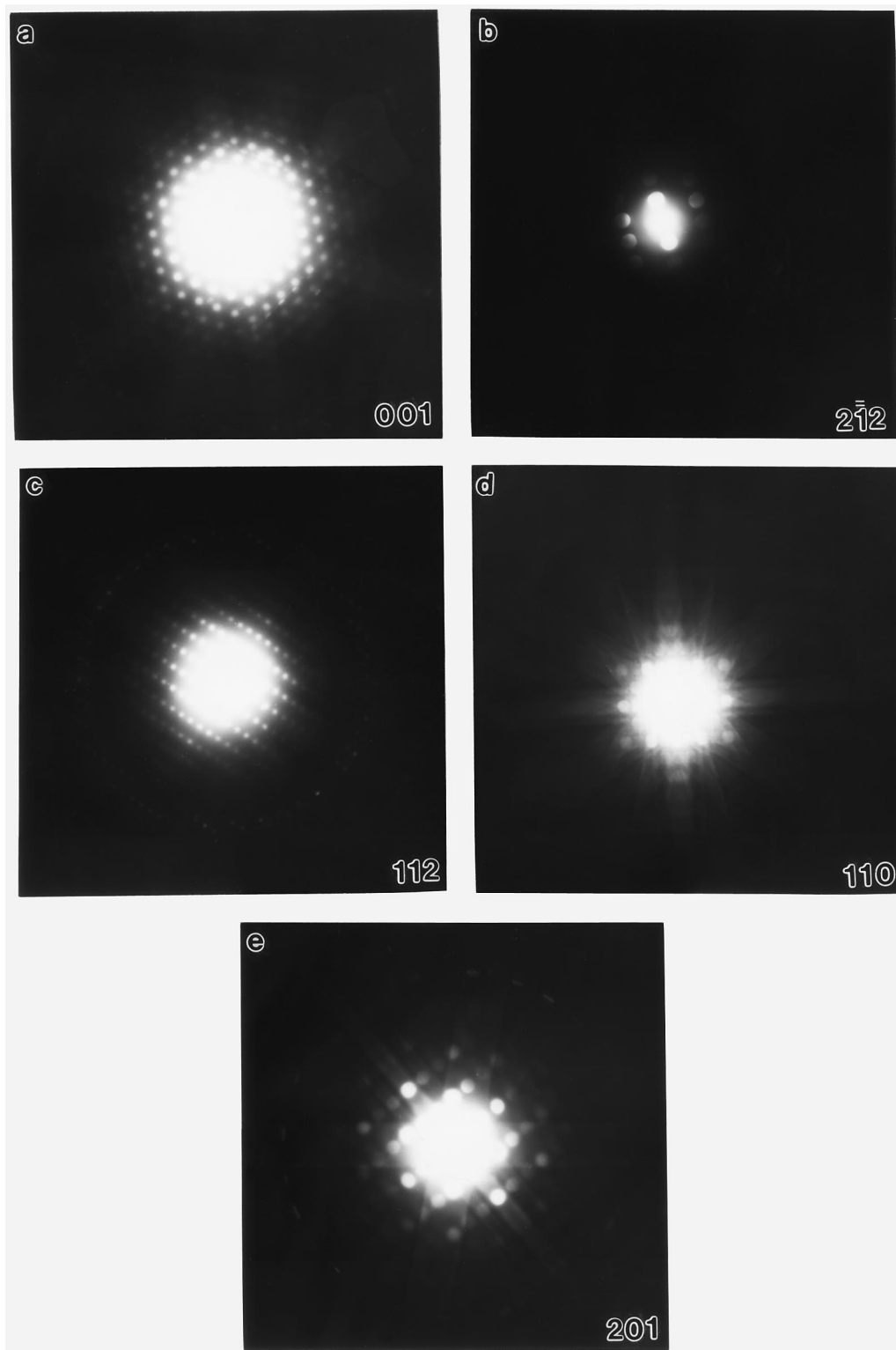


Fig. 7—CBED pattern obtained from reaction product: (a) AlN and (c) MgAl₂O₄ in the control alloy and (b) AlN, (d) MgAl₂O₄, and (e) AlB₂ in the composite.

alloy by means of an enhancement of wetting between molten alloy and reinforcement. However, the authors did not present either direct or indirect evidence on this suggestion. The overall reactions are summarized as follows:

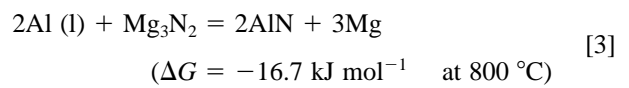
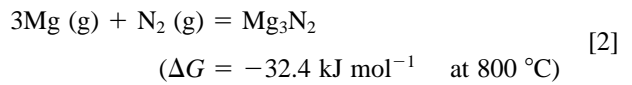


Table I. Analytical Results of CBED Pattern Obtained from Reaction Products

Specimen	Primitive Cell Volume (\AA^3)		Height of Reciprocal Lattice (\AA^{-1})			Result
	Experimental	Theoretical	Experimental	Theoretical	Zone Axis	
Control alloy	45.16	41.74	0.2008	0.1917	[001]	AlN, hexagonal
Composite	44.05	41.74	0.774	0.07581	[2T2]	AlN, hexagonal
Control alloy	132.55	132.03	0.1010	0.1005	[112]	MgAl ₂ O ₄ , cubic
Composite	139.04	132.03	0.1749	0.1736	[110]	MgAl ₂ O ₄ , cubic
Composite	29.5013	25.44	0.1463	0.14291	[201]	AlB ₂ , hexagonal

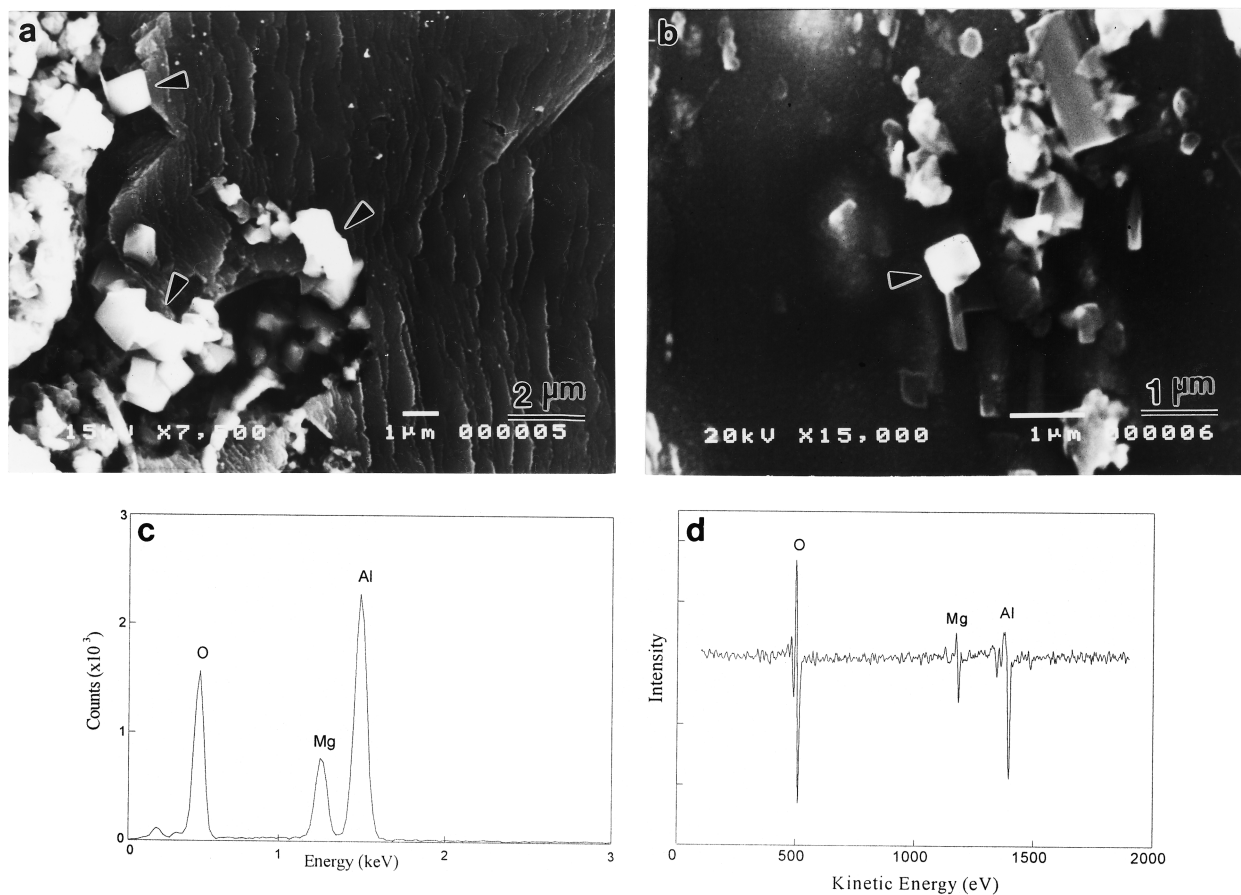


Fig. 8—SEM micrographs, EDS, and AES spectra showing MgAl₂O₄ after dissolving away the Al alloy matrix: (a) control alloy and (b) composite.

Recently, Lee and Kwon^[20] indirectly demonstrated that the formation of Mg₃N₂ is necessary to induce spontaneous infiltration. In their model experiment, an assembly with Mg similar to Figure 1 and another one without Mg were simultaneously placed into a retort furnace and heated under a nitrogen atmosphere. However, the spontaneous infiltration occurred even in the assembly without Mg. In a separate experiment, where only a single assembly without Mg was used, spontaneous infiltration did not occur, even though there was a nitrogen atmosphere. Thus, the Mg in one assembly with Mg forms Mg₃N₂, and this Mg₃N₂ flows into the other assembly without Mg, resulting in spontaneous infiltration.

The hypothesis is, therefore, that when molten Al comes into contact with Mg₃N₂, this compound decomposes, resulting in the formation of AlN (Reaction [3]). Hou *et al.*^[25] and Kobashi *et al.*^[26] reported that molten Al infiltrated

into Mg₃N₂ powders spontaneously; AlN was synthesized as a result of the *in-situ* reaction.

If we find the sites of AlN formation in the control alloy without ceramic particles where there are no severe interfacial reactions at the ceramic surface, we thus can identify the sites of prior Mg₃N₂ formation. As shown in Figures 3 and 4, the original sites of AlN formation in the control alloy were the surfaces of the old Al particles in powder bed. Therefore, the spontaneous infiltration results from the great enhancement of wetting through the Mg₃N₂ formation on the surfaces of Al particles comprising the powder bed.

Even though we could not directly observe Mg₃N₂ inside the composite and control alloy after completing the infiltration due to Reaction [3], a greenish-yellow powder was frequently observed on the fabricated composite surface and on the retort wall. This powder was transferred to the SEM as soon as possible and analyzed by EDS; its composition

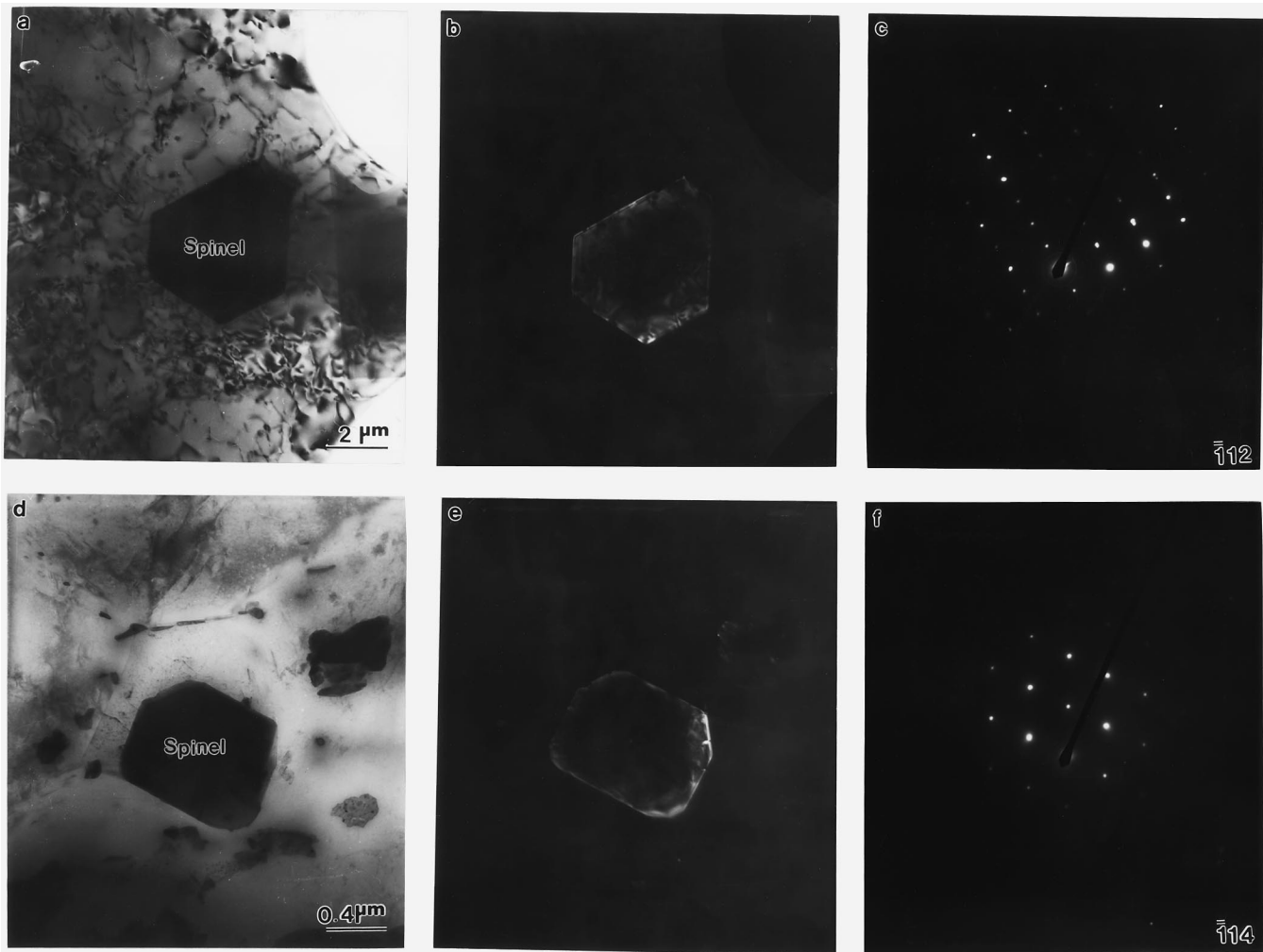


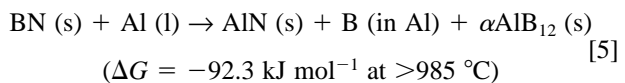
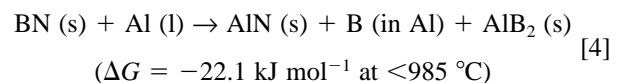
Fig. 9—TEM micrographs showing reaction product, $MgAl_2O_4$: (a) BF, (b) DF, and (c) SADP in control alloy and (d) BF, (e) DF, and (f) SADP in the composite.

nearly coincided with that of Mg_3N_2 .^[19] In addition, when the fabricated composite was immersed in water, it smelled like ammonia; $Mg_3N_2 + 6H_2O = 3Mg(OH)_2 + 2NH_3$.^[27,28] However, since the reason why the Mg_3N_2 induces the spontaneous infiltration of molten Al has not been clearly established, various model experiments to identify the role of Mg_3N_2 are currently in progress.

From the preceding analysis, the spontaneous infiltration behavior is summarized in a schematic diagram in Figure 15.

B. Strengthening Behavior

Fine AlN particles formed *in situ* led to a significant enhancement of strength in the control AA6061. As shown in Figure 3, the AlN peak intensities were much higher in the composite, compared with those observed in the control AA6061. This result indicates that the amount of AlN formed in the composite greatly increased when compared to the control AA6061. This is due to the AlN formed both through the interfacial reaction at the interfaces of BN/Al alloy melt as well as *in situ*, as previously mentioned. An interfacial reaction between BN and Al melt is described as follows:^[13]



There were many reports showing the AlN was formed by the reaction between Al and BN.^[11–16] Therefore, a further increase in the strength of the composite is attributed to both the addition of BN and the increase in the amount of AlN particles through the additional reaction at BN/Al alloy melt interface, as compared to the control alloy. In addition, αAlB_{12} or AlB_2 can be formed by the interfacial reaction in the BN/Al system. However, in the present composite fabricated at 800°C, only AlB_2 was observed, as illustrated in Figures 10 and 11. This is coincident with Reaction [4] at temperatures below 985 °C. Also, the influence of this phase on the strength seems to be negligible due to its small amount and to its excessively large size.

Next, when BN reinforced composite is compared with a Si_3N_4 reinforced composite^[20] (Table II), an interesting point may be indicated. The volume fraction of ceramic particles in the powder bed prior to infiltration is 5 and 10

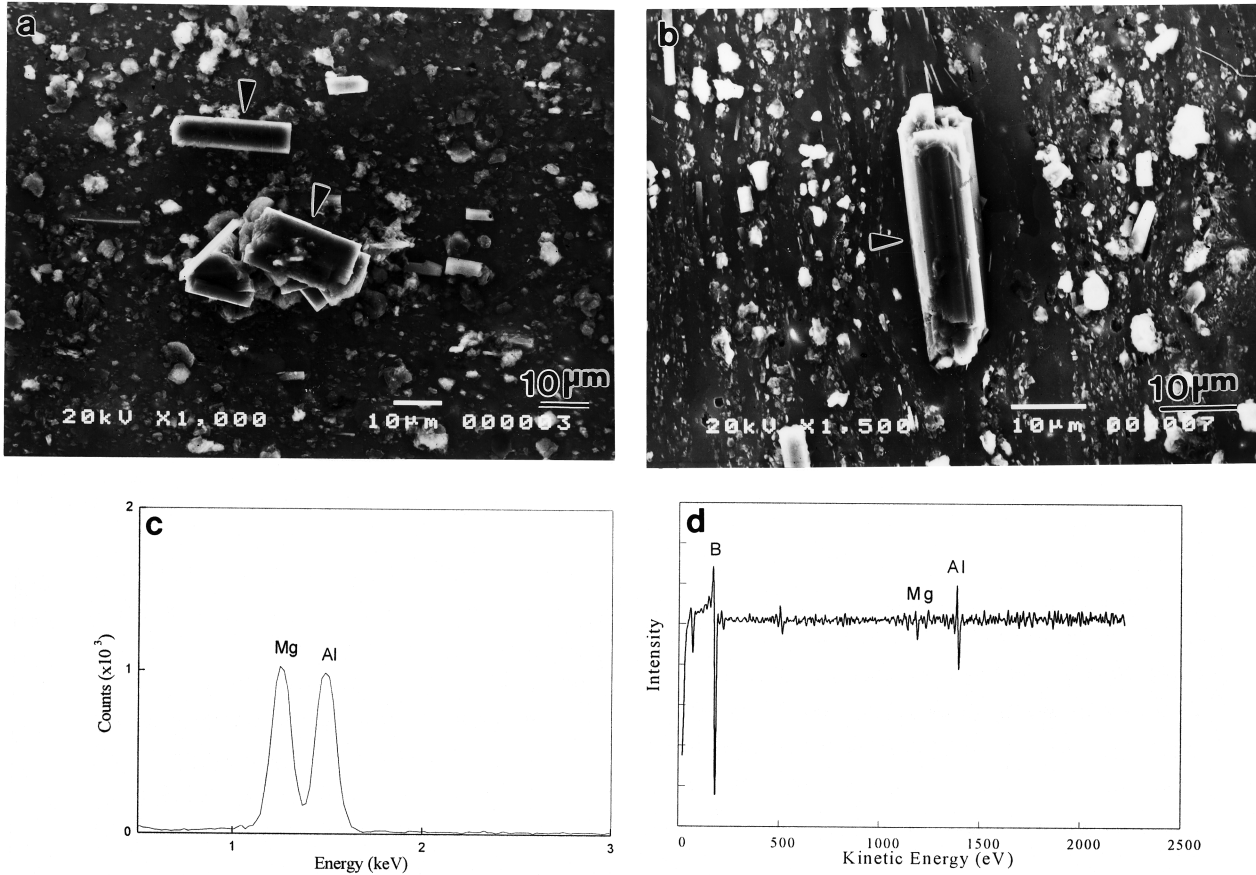


Fig. 10—(a) through (d) SEM micrographs, EDS, and AES spectra showing AlB_2 after dissolving away the Al alloy matrix in the composite.

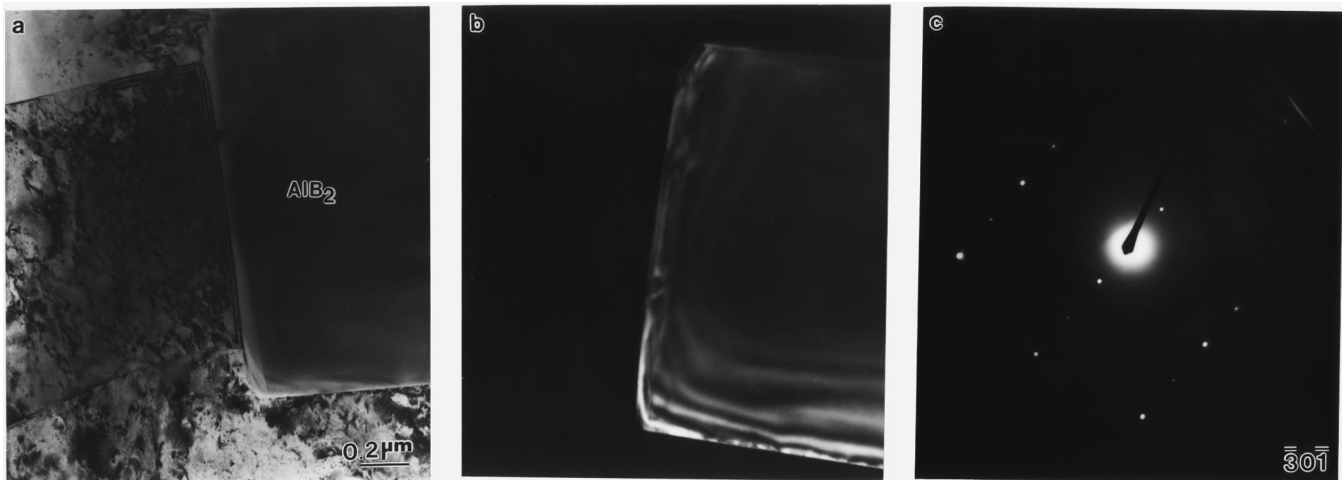


Fig. 11—TEM micrographs showing the reaction product, AlB_2 , in the composite: (a) BF (b) DF, and (c) SADP.

pct in the BN and Si_3N_4 reinforced composites, respectively. However, the strengthening effect is the opposite of the general concept that a higher volume fraction of reinforcement leads to more strengthening. In other words, the increase in strength in the case of the former composite with lower volume fraction was higher than in the case of the latter one, as compared to the control alloy. In the case of tensile strength, the relative increases in the BN and Si_3N_4 reinforced composites were 50 to 90 and 35 to 55 MPa, respectively.

At present, this opposite effect may be considered in terms of its two main aspects, the difference in the amount of AlN and the difference in the strengthening behavior due to the particle morphology. If it is assumed that the amount of AlN formed *in situ* is the same in both composites, the amount of AlN formed through the interfacial reaction may be larger in the BN reinforced composite. In reality, the higher peaks of AlN in the XRD spectra were observed in the BN reinforced composite. Next, while the Si_3N_4 particles have the polyhedron shape (average size 1 μm), the BN particles

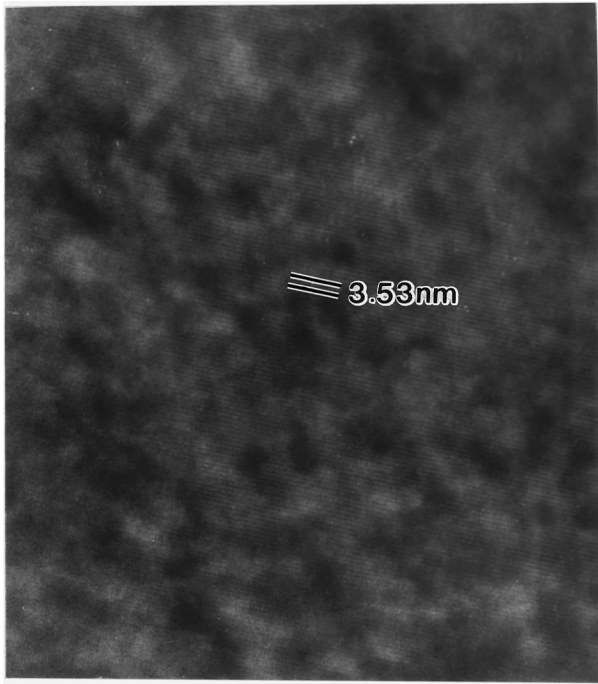


Fig. 12—HRTEM micrograph showing lattice image of the reaction product, AlB_2 .

have the flake shape (average thickness $0.8\ \mu\text{m}$ and average diagonal length $8\ \mu\text{m}$). Since after extrusion, the flakes are aligned to working direction, they present a specific strong hardening effect similar to discs with an aspect ratio of 10.

Finally, the grain size was measured by the linear intercept method in order to investigate its effect on the strength of the materials. The grain size of the control alloy is decreased significantly to about $20\ \mu\text{m}$, compared to $50\ \mu\text{m}$ for the commercial alloy. In addition, the grain size in the composite reinforced with BN is further decreased to about $3.0\ \mu\text{m}$. These grain refinements contributed to strengthening of the control alloy and of the composite as well. It is well known that in particle-reinforced MMCs, the grain size is generally small compared to an unreinforced material of similar composition, and it has been shown that particle-stimulated

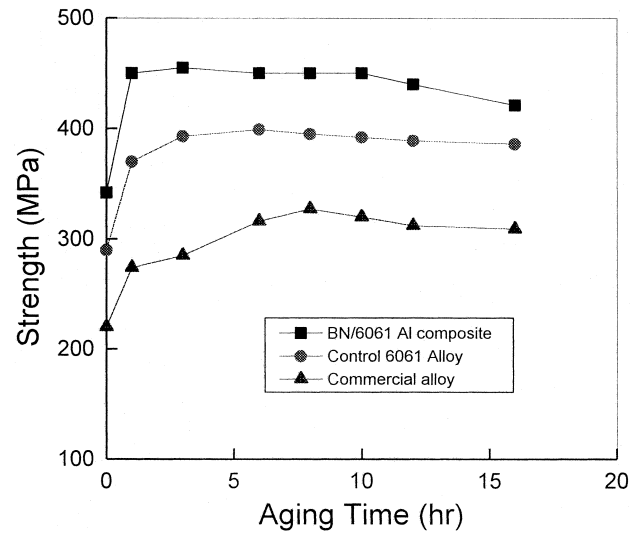


Fig. 14—Tensile strength variation with aging time after a solution heat treatment of 2 h at $529\ ^\circ\text{C}$.

nucleation, coupled with particle pinning during normal grain growth, is responsible for this small grain size.^[29,30]

V. CONCLUSIONS

1. The Mg_3N_2 formed in the presence of Mg vapor and nitrogen gas, which coated the particles in the powder bed, induces spontaneous infiltration through an enhancement of wetting by the following reaction: $\text{Mg}_3\text{N}_2 + 2\text{Al} \rightarrow 2\text{AlN} + 3\text{Mg}$. This was identified by finding AlN particle layers on the surfaces of prior Al particles in the powder bed that came into contact with the infiltrating melt. In addition, unreacted Mg_3N_2 was observed outside the composite, where the Al melt did not come into direct contact.
2. The main reaction product was the AlN formed *in situ* in both the control alloy and the composite. In the composite reinforced with BN, additional AlN was formed by the interfacial reaction between BN and Al melt as well as by the *in-situ* reaction. An additional reaction product

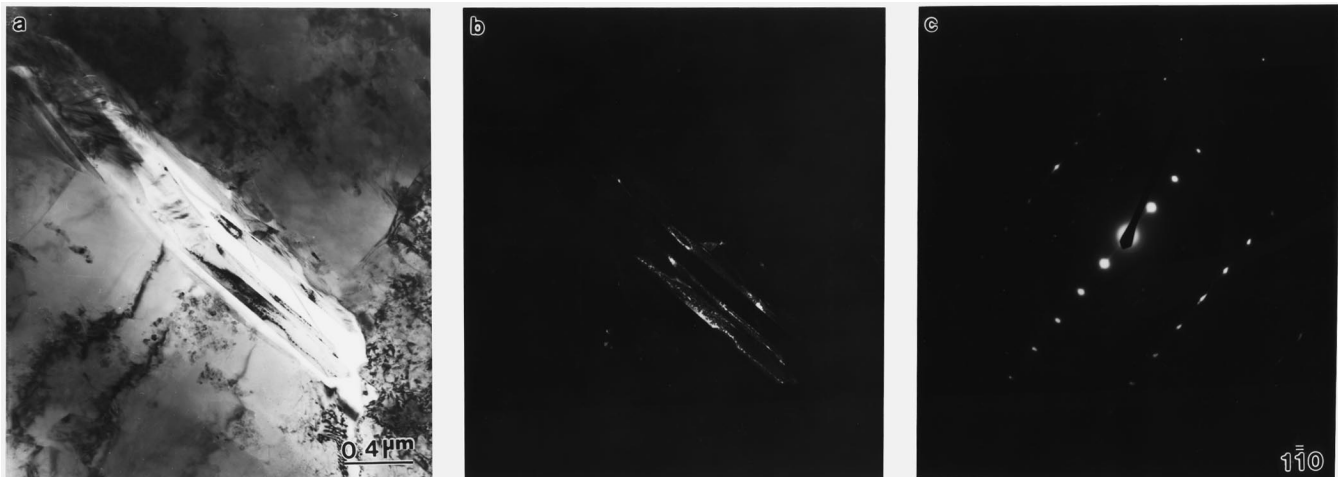


Fig. 13—(a) through (c) TEM micrographs showing BN morphology.

Table II. Tensile Properties of 6061 Al, Control Alloy, and Composites

Material Designations	UTS (MPa)		YS (MPa)		El (Pct)	
	ST	T6	ST	T6	ST	T6
Commercial AA6061	220	312	104	271	15.1	6.8
Control AA6061	290	367	209	323	10.8	6.2
AA6061/BN(5 vol pct) composite	342	455	265	428	11.0	4.7
AA6061/Si ₃ N ₄ (10 vol pct) composite ^[20]	327	422	241	406	6.5	1.5

UTS: ultimate tensile strength, YS: 0.2 pct offset yield strength, El: elongation, and ST: solution-treated condition.

Table III. Contact Angle between BN and Al

797 °C	900 °C	1000 °C	1100 °C	Atmosphere	Reference
—	—	—	<90	unknown	24
160	158	90	35	vacuum	17
151	139	50	—	vacuum	18
151	122*	72**	34†	vacuum	14
—	127	0	0	vacuum	13

*917 °C
**1007 °C
†1107 °C

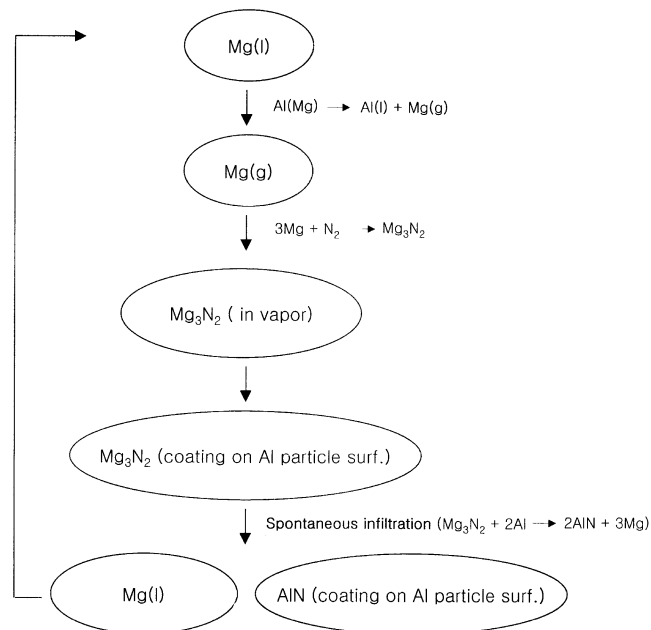


Fig. 15—Summary on the spontaneous infiltration behavior.

observed in both control alloy and composite was MgAl₂O₄ spinel. Another reaction product, AlB₂ was formed by the interfacial reaction of the BN and Al melt in the composite.

- A significant strengthening even in the control alloy occurred due to the formation of *in-situ* AlN particles even without an addition of BN particles. A further strengthening of the composite was produced by the reinforced BN particles and the AlN particles additionally formed by means of the interfacial reaction, as compared to the control alloy with only *in-situ* strengthening.
- The grain size of the control alloy significantly decreased to about 20 μm compared to 50 μm for the commercial

alloy. In addition, the grain size in the composite reinforced with BN further decreased to about 3.0 μm. This grain refinement contributed to strengthening of the control alloy and composite.

- The flake shape of the BN particles exhibited additional strengthening, compared with spherical particles, such as Si₃N₄. This may be attributable to a higher aspect ratio of the flake shape.

ACKNOWLEDGMENTS

This work was supported by the Ministry of Education, Research Fund for Advanced Materials, 1997.

REFERENCES

- A. Mortensen and I. Jin: *Int. Mater. Rev.*, 1992, vol. 37, pp. 101-28.
- A. Ibrahim, F.A. Mohamed, and E.S. Lavernia: *J. Mater. Sci.*, 1991, vol. 26, pp. 1137-56.
- M.J. Koczak and M.K. Premkumar: *J. Metall.*, 1993, vol. 45, pp. 44-48.
- R. Asthana: *J. Mater. Sci.*, 1998, vol. 33, pp. 1679-98.
- M.K. Aghajanian, J.T. Burke, D.R. White, and A.S. Nagelberg: *SAMPE Q.*, 1989, vol. 20 (4), pp. 43-6.
- M.K. Aghajanian, M.A. Rocazella, J.T. Burke, and S.D. Keck: *J. Mater. Sci.*, 1991, vol. 6, pp. 447-54.
- A.W. Urquhart: *Adv. Mater. Process.*, 1991, July, pp. 25-29.
- A.W. Urquhart: *Mater. Sci. Eng.*, 1991, vol. A144, pp. 75-82.
- R.E. Everett and R.J. Arsenault: *Metal Matrix Composites: Processing and Interfaces*, Academic Press, New York, NY, 1991, pp. 121-50.
- M.K. Aghajanian, A.S. Nagelberg, and C.R. Kennedy: U.S. Patent 5020584, 1991.
- X.M. Xue, J.T. Wang, and M.X. Quan: *J. Mater. Eng.*, 1991, vol. A132, pp. 277-80.
- L. Shen, B.J. Tan, W.S. Willis, F.S. Galasso, and S.L. Suib: *J. Am. Ceram. Soc.*, 1994, vol. 77, pp. 1011-16.
- H. Fujii, H. Nakae, and K. Okada: *Acta. Metall. Mater.*, 1993, vol. 41, pp. 2963-71.
- X.M. Xue, J.T. Wang, and M.X. Quan: *J. Mater. Sci.*, 1991, vol. 26, pp. 6391-95.
- X.M. Xue, J.T. Wang, and F.M. Zhao: *J. Mater. Sci. Lett.*, 1992, vol. 11, pp. 199-201.
- M. Kobashi and T. Choh: *J. Mater. Sci.*, 1997, vol. 32, pp. 6283-89.
- M.G. Nicholas, D.A. Mortimer, L.M. Jones, and R.M. Crispin: *J. Mater. Sci.*, 1990, vol. 25, pp. 2679-89.
- F.P. Chiamonte and B.N. Rosenthal: *J. Am. Ceram. Soc.*, 1991, vol. 74, pp. 658-61.
- K.B. Lee, Y.S. Kim and H. Kwon: *Metall. Mater. Trans. A*, 1998, vol. 29A, pp. 3087-95.
- K.B. Lee and H. Kwon: *Metall. Mater. Trans. A*, 1999, vol. 30A, pp. 2999-3007.
- K.B. Lee, H.S. Sim, S.W. Heo, S.Y. Cho, and H. Kwon: *Kor. Inst. Metall. Mater.*, 2000, vol. 6, pp. 25-32.
- CRC Materials Science and Engineering Handbook*, J.F. Shackelford, W. Alexander, and J.S. Park, eds., CRC, Boca Raton, FL, 1994, p. 43.
- J.C. Viala, G. Gonzales, and J. Bouix: *J. Mater. Sci. Lett.*, 1992, vol. 11, pp. 711-4.
- Y. Naidich: *Progr. Surf. Membrane Sci.*, 1981, vol. 14, p. 353.

25. Q. Hou, R. Mutharasan, and M. Koczak: in *In Situ Reactions for Synthesis of Composites, Ceramics, and Intermetallics*, E.V. Barrera, F.D.S. Marquis, W.E. Frazier, S.G. Fishman, N.N. Thadhani, and Z.A. Munir, eds., TMS-AIME, Warrendale, PA, 1995, pp. 45-55.
26. M. Kobashi, N. Okayama, and T. Choh: *Mater. Trans. JIM*, 1997, vol. 38, pp. 60-65.
27. I.S. Gladkaya, G.N. Kremkova, and N.A. Bendeliani: *J. Mater. Sci. Lett.*, 1993, vol. 12, pp. 1547-48.
28. T. Murata, K. Itatani, F.S. Howell, A. Kishioka, and M. Kinoshita: *J. Am. Ceram. Soc.*, 1993, vol. 76, pp. 2909-11.
29. F.J. Humphreys, W.S. Miller, and M.R. Djazeb: *Mater. Sci. Technol.*, 1990, vol. 6, pp. 1157-66
30. M. Ferry, P. Monroe, A. Crosky, and T. Chandra: *Mater. Sci. Technol.*, 1992, vol. 8, pp. 43-51.